HHS Public Access

Author manuscript

Nat Neurosci. Author manuscript; available in PMC 2016 March 01.

Published in final edited form as:

Nat Neurosci. 2015 September ; 18(9): 1226–1229. doi:10.1038/nn.4085.

Modifiers of *C9orf72* DPR toxicity implicate nucleocytoplasmic transport impairments in c9FTD/ALS

Ana Jovičić[1], **Jerome Mertens**[2], **Steven Boeynaems**[3,4], **Elke Bogaert**[3,4], **Noori Chai**[1,5], **Shizuka B. Yamada**[1,6], **Joseph W. Paul III**[1], **Shuying Sun**[7], **Joseph R. Herdy**[4], **Gregor Bieri**[1,5], **Nicholas J. Kramer**[1,5], **Fred H. Gage**[2], **Ludo Van Den Bosch**[3,4], **Wim Robberecht**[3,4,8], and **Aaron D. Gitler**[1,9]

[1]Department of Genetics, Stanford University School of Medicine, Stanford, CA 94305

[2]Salk Institute for Biological Studies, Sanford Consortium for Regenerative Medicine, La Jolla, CA 92037

[3]KU Leuven - University of Leuven, Department of Neurosciences, Experimental Neurology and Leuven Research Institute for Neuroscience and Disease (LIND), B-3000 Leuven, Belgium

[4]VIB, Vesalius Research Center, Laboratory of Neurobiology, B-3000 Leuven, Belgium

[5]Neuroscience Graduate Program, Stanford University School of Medicine, Stanford, CA 94305

[6]Department of Biology, Stanford University, Stanford, CA 94305

[7]Ludwig Institute for Cancer Research, Departments of Cellular and Molecular Medicine and of Neurosciences, University of California at San Diego, La Jolla, CA 92093

[8]University Hospitals Leuven, Department of Neurology, B-3000 Leuven, Belgium

Abstract

C9orf72 mutations are the most common cause of amyotrophic lateral sclerosis (ALS) and frontotemporal dementia (FTD). Dipeptide repeat proteins (DPRs) produced by unconventional translation of the *C9orf72* repeat expansions cause neurodegeneration in cell culture and in animal models. We performed two unbiased screens in *Saccharomyces cerevisiae* and identified potent modifiers of DPR toxicity, uncovering karyopherins and effectors of Ran-mediated nucleocytoplasmic transport, providing insight into potential disease mechanisms and therapeutic targets.

[9]Correspondence should be addressed to: A.D.G, Aaron D. Gitler, 300 Pasteur Drive, M322 Alway Building, Stanford, CA 94305, 650-725-6991 (phone), agitler@stanford.edu.

Author Contributions

A.J. designed and performed the yeast experiments with help from N.C., S.B.Y., J.W.P., G.B., and N.J.K. S.B. and E.B. generated and characterized some yeast expression plasmids with direction from L.V.D.B. and W.R. A.J. performed the mouse primary neuron experiments. A.J., S.S., J.M., J.R.H. worked together on the human iPS neuron experiments with direction from F.H.G. A.J. and A.D.G. wrote the manuscript with input from all authors.

Competing financial interests

The authors declare no competing financial interests.

The *C9orf72* gene contains a polymorphic hexanucleotide repeat, GGGGCC, located in an intron. In c9FTD/ALS cases, the hexanucleotide repeat tract is expanded to hundreds or even thousands of repeats[1,2]. An exciting hypothesis has emerged to explain how GGGGCC repeat expansion in *C9orf72* could cause disease: repeat-associated non-ATG (RAN) translation. This unconventional form of translation occurs in all reading frames (sense and antisense directions) of the expanded GGGGCC nucleotide repeat, producing polymers of the predicted dipeptides: glycine-alanine (GA), glycine-proline (GP), proline-alanine (PA), glycine-arginine (GR), and proline-arginine (PR). These dipeptide repeat proteins (DPRs) are themselves aggregation-prone and accumulate in the central nervous system of affected *C9orf72* mutation carriers[3–5]. But does pathology = pathogenesis? In other words, are these DPRs toxic and cause neurodegeneration or are they merely benign bystanders? If they are toxic, then defining the mechanisms by which they contribute to neurodegeneration will provide strategies for therapeutic intervention.

Several groups recently reported experiments demonstrating that *C9orf72* DPRs are toxic and can cause neurodegeneration[5–11]. The arginine-rich DPRs, GR and PR, seem to be particularly toxic[6,7,11]. Now, the big challenge is to define the cellular pathways affected by the toxic *C9orf72* DPRs. We have previously used yeast as a model system to gain insight into other ALS disease proteins, including TDP-43 and FUS[12–14]. To investigate potential toxicity of *C9orf72* DPRs in yeast, we expressed constructs harboring 50 repeats of four of the five different predicted DPRs (GA, GR, PA, PR) under the control of a strong inducible promoter (galactose-inducible promoter). To focus specifically on DPR toxicity and not RNA-related toxicity, we generated codon-optimized constructs to express each DPR independently, without using the GGGGCC repetitive sequence. We transformed these constructs into wild type yeast cells and assessed the effects on growth using spotting assays. Strikingly consistent with the results in *Drosophila* and mammalian cells, the arginine-rich DPRs were toxic, with $(PR)_{50}$ expression in particular leading to highest levels of toxicity (Fig. 1a and Supplementary Fig. 1a). $(GR)_{50}$ was less toxic in yeast than $(PR)_{50}$ (Fig. 1 a,b). Increasing the number of GR repeats to 100 ($(GR)_{100}$) increased toxicity (Fig. 1b). Thus, this simple yeast model recapitulates arginine-rich *C9orf72* DPR toxicity.

To gain insight into the mechanisms of *C9orf72* pathogenesis, we used an unbiased genetic approach to identify genes that could suppress or enhance DPR toxicity in yeast. We focused on PR because of its robust toxicity and because it elicited toxicity and neurodegeneration in mammalian cells and *Drosophila*[6,7,11]. We performed two complementary genomewide screens. First, we performed a genomewide plasmid overexpression screen (Fig. 1c). We individually transformed 5,500 yeast genes, which comprise the yeast FLEXGene plasmid library, into a yeast strain expressing $(PR)_{50}$. We identified genes that either suppressed or enhanced $(PR)_{50}$ toxicity (i.e., allow the cells to grow better or worse in the presence of $(PR)_{50}$ expression) (Fig. 1d). We repeated the screen two independent times and verified any potential hits at least 3 additional times with independent transformations and spotting assays. We identified 27 $(PR)_{50}$ toxicity suppressors and 35 enhancers (Table 1). We performed immunocytochemistry and immunoblotting to define the impact of the modifiers on $(PR)_{50}$ localization and expression levels (see Online Methods and Supplementary Fig. 1b,c).

Next, to complement the plasmid overexpression screen, we also screened a library of all 4,850 non-essential yeast gene knockouts to identify deletions that could suppress $(PR)_{50}$ toxicity (Fig. 1e). Hits from this screen are a particularly interesting class of modifiers (gene deletions that suppress a phenotype) because they could represent potential drug targets. We identified 16 yeast genes that suppressed $(PR)_{50}$ toxicity when deleted (Table 2). That is, deletions of these genes improved the growth of yeast cells expressing $(PR)_{50}$, which is extremely toxic on its own. Some of these deletions seem to nearly completely suppress $(PR)_{50}$ toxicity (Fig. 1f and Supplementary Figs. 1 c,d and 2 a,b).

Combining the results from both gain- and loss-of-function screens, we found a striking enrichment in genes functioning in nucleocytoplasmic transport using gene ontology analysis (P=5.9E^{-4}) (Fig. 1g). Six of the strongest modifier genes from the plasmid overexpression screen encode highly conserved members of the karyopherin family of nuclear import proteins (Fig. 1d). We performed immunocytochemistry to define the impact of the karyopherins on $(PR)_{50}$ localization. Upregulation of karyopherins rescued toxicity but did not alter localization or levels of the DPRs (Supplementary Fig. 1 b,c). Thus, the DPRs could interfere with nucleocytoplasmic transport *per se* (perhaps by interacting with karyopherin proteins or the nuclear pore directly), rather than specifically affecting the localization of the DPRs.

We identified yeast *MTR10* as a suppressor of $(PR)_{50}$ toxicity. Mtr10p is an import receptor, which mediates the nuclear import of SR proteins and their bound mRNAs and RNA-binding proteins[15]. It has been proposed that arginine-rich *C9orf72* DPRs compete with SR proteins for binding to ribonucleoprotein granules[7]. Our genetic results suggest a possible way to overcome this blockade by upregulating the SR protein import receptor. We also identified *KAP104*, the yeast homolog of karyopherin β2 (also called transportin 1), which mediates nuclear import of the ALS disease protein FUS/TLS (Fig. 1d). ALS-associated mutations in the FUS/TLS nuclear localization signal (NLS) are known to disrupt karyopherin β2-mediated nuclear import[16] and disturbances in nuclear import are a pathological feature of FTD cases with FUS pathology (FTD-FUS)[17].

Because upregulation of yeast karyopherin genes were among the strongest suppressors of $(PR)_{50}$ toxicity in our yeast screen, it suggests that strategies to boost production or enhance function of karyopherin proteins could be a therapeutic strategy to protect against *C9orf72* DPR proteotoxicity. We performed experiments to rescue $(PR)_{50}$ toxicity in primary rodent neurons with *KPNA3* (human homolog of yeast *KAP122*, one of the strongest upregulation suppressors of $(PR)_{50}$ toxicity). We used lentivirus to infect rodent primary cortical neurons with a construct expressing $(PR)_{50}$. This was highly toxic, consistent with previous reports (Fig. 3a). Co-infection with a lentivirus encoding *KPNA3* more than doubled the survival of neurons expressing $(PR)_{50}$, compared to co-infection with a GFP-expressing virus (Fig. 1h). *KPNA3* upregulation did not affect the levels or distribution of $(PR)_{50}$ (Supplementary Fig. 3) and did not completely rescue toxicity; consistent with other modifiers (e.g., additional karyopherins or even other pathways) probably contributing to toxicity.

Beyond karyopherins, we identified other genetic modifiers that underscore nuclear import and export as a critical target of DPRs (Fig. 1g). These include *NDC1*, a key component of

the nuclear pore complex, and regulators of the Ran-GTPase cycle, which generates the energy to power nuclear import. Upregulation of *SRM1*, the yeast homolog of human *RCC1*, the ran guanine-nucleotide exchange factor, enhanced $(PR)_{50}$ toxicity. Targeting this regulator may permit modulation of Ran-GTP levels to overcome nuclear transport defects caused by *C9orf72* DPRs.

Our genetic results are consistent with arginine-rich *C9orf72* DPRs disrupting nucleocytoplasmic transport. As a first step to validate this result in human disease, we next analyzed neurons derived from 3 control subjects and 2 *C9orf72* mutation carriers. We directly converted fibroblasts into neurons (induced neurons; iNs) using proneural transcription factors *Ngn2* and *Ascl1*, similar to previously described methods[18]. We examined the integrity of nucleocytoplasmic transport in human iNs by quantifying the nuclear/cytoplasmic localization of RCC1, a Ran guanine nucleotide exchange factor. RCC1 is the human homolog of SRM1 identified in our overexpression screen as an enhancer of $(PR)_{50}$ toxicity. In control iNs, RCC1 was strongly localized to the nucleus. However, 70–80% of the *C9orf72*-carrier iNs had either no or only very weak nuclear RCC1 compared to cytoplasmic staining (Fig. 1 i,j). We also examined the localization of five other proteins implicated in nucleocytoplasmic transport (LmnB, TPNO3, KPNA3, RanGap1, and XPO5), but did not observe major differences in *C9orf72*-carrier iNs compared to controls (Supplementary Fig. 4). Future studies will be required to further define the effect of *C9orf72* mutations on nucleocytoplasmic transport in human cells and in animal models[19].

In addition to the nuclear import and export proteins, we identified several genes involved in ribosomal RNA (rRNA) processing as potent modifiers of PR toxicity. Dramatic disruptions in rRNA biogenesis by *C9orf72* DPRs have previously been reported[7,20] but whether these defects were cause or consequence of DPR toxicity was unclear. Our data demonstrating potent rescue of DPR toxicity by genetic manipulation of rRNA processing machinery indicate that rRNA processing pathway alterations are a critical component of DPR toxicity and, importantly, can be overcome by restoring rRNA processing machinery function. Intriguingly, we identified *NSR1* as a strong modifier of $(PR)_{50}$ toxicity – deletion suppressed toxicity (Table 2) and upregulation enhanced toxicity (Table 1). *NSR1* encodes the yeast homolog of human nucleolin, a nucleolar protein whose disruption has been recently implicated in c9FTD/ALS pathogenesis[20].

Because the arginine-rich DPRs GR and PR may promote toxicity through a common pathway, we next examined the effects of some of the strongest $(PR)_{50}$ toxicity modifiers in yeast expressing GR. We tested 12 of 16 deletion suppressors from the $(PR)_{50}$ screen and 11 out of 12 of these suppressed $(GR)_{100}$ toxicity (Table 2). $(GR)_{100}$ toxicity in the W303 strain background was not sufficient to test the suppressors and enhancers from the overexpression screen (data not shown). Future comprehensive screens for modifiers of $(GR)_{100}$ toxicity (as well as the other DPRs, such as GA, GP, and PA) will hopefully provide even further insight into shared and distinct mechanisms of DPR toxicity.

Using two unbiased genetic screens in yeast, we identified a network of potent modifiers of *C9orf72* DPR toxicity. These modifiers, especially the gene deletions that suppress toxicity, could point to a druggable target that antagonizes DPR toxicity in c9FTD/ALS. Beyond

potential drug targets, the modifiers suggest hypotheses about mechanisms of DPR toxicity (e.g., impairments in nucleocytoplasmic transport (both import and export; Fig. 1g).

Online Methods

Yeast Strains, Media, and Plasmids

Yeast cells were grown in rich media (YPD) or in synthetic media lacking uracil and containing 2% glucose (SD-Ura), raffinose (SRaf-Ura), or galactose (SGal-Ura). To generate *C9orf72* dipeptide expression constructs $(PR)_{50}$, $(PA)_{50}$, $(GA)_{50}$ and $(GR)_{50}$ we utilized codon-optimized DPR sequences using Mfold software to minimize the formation of stable RNA secondary structures. ATG-DPR-FLAG constructs were synthesized by Genscript (Piscataway, USA) and were flanked by attB sites. Constructs were further subcloned into a pDONR221 plasmid and subsequently used in Gateway LR reactions with pAG416GAL-ccdB or pAG303GAL-ccdB to produce yeast expression vectors. All constructs were verified by DNA sequencing. pAG416GAL-DPR constructs were transformed into Y7092 strain. pAG303GAL-DPR constructs were transformed into W303 strain. Strains were manipulated and media prepared using standard techniques.

Yeast transformation and spotting assays

Yeast procedures were performed according to standard protocols. We used the PEG/lithium acetate method to transform yeast with plasmid DNA. For spotting assays, yeast cells were grown overnight at 30°C in liquid media containing SRaf-Ura until they reached log or mid-long phase. Cultures were then normalized for OD_{600}, serially diluted and spotted with a Frogger (V&P Scientific) onto synthetic solid media containing glucose (SD-Ura) or galactose (SGal-Ura) lacking uracil and were grown at 30°C for 2–3 days.

Yeast Genetic screens

The yeast FLEXGene collection was used to perform the genome-wide plasmid overexpression screen[21]. Plasmid DNA from the expression clones were isolated using the Plasmid *Plus* 96 miniprep kit (Qiagen). DNA was dried in individual wells of 96-well microtiter plates and transformed into a strain expressing $(PR)_{50}$ integrated at the HIS3 locus. A standard lithium acetate transformation protocol was modified for automation and used by employing a BIOROBOT Rapidplate 96-well pipettor (Qiagen). The transformants were grown in synthetic deficient media lacking uracil (SD-Ura) with glucose overnight. The overnight cultures were inoculated into fresh SD-Ura media with raffinose and allowed to reach stationary phase. The cells were spotted on to SD-Ura + glucose and SD-Ura + galactose agar plates. Suppressors of $(PR)_{50}$ induced toxicity were identified on galactose plates after 2–3 days of growth at 30°C. We repeated the screen two independent times and candidate modifier genes were retested at least three times to confirm their authenticity. To exclude false-positive enhancer genes caused by a general inhibition of growth unrelated to $(PR)_{50}$ expression, these genes were transformed into wild type yeast cells and their effect on growth determined.

We used synthetic genetic array (SGA) analysis to identify nonessential yeast deletions that modify *C9orf72* dipeptide toxicity. We performed this screen essentially as described in[22],

with some modifications using a Singer RoToR HAD (Singer Instruments). We mated MATα strain expressing $(PR)_{50}$ dipeptide under galactose promoter to the yeast haploid deletion collection of nonessential genes (MATa, each gene deleted with KanMX cassette conferring resistance to G418). Following diploid selection and sporulation, we selected haploids carrying both deletion and $(PR)_{50}$ expression cassette. Colony sizes were measured using the ht-colony-measurer software[23]. The raw values were normalized by dividing them by the median colony size of the plate. We performed the entire screen two independent times and confirmed each of the candidate modifier genes at least two times to confirm their authenticity.

We tested effects of the deletions on $(PR)_{50}$ expression levels. Some modifiers lowered levels of $(PR)_{50}$ (e.g., *dhh1*Δ, *gtr1*Δ, *sgo1*Δ, *ski8*Δ, *stp1*Δ and *uaf30*Δ) (Supplementary Fig. 1c). Deletion of these 6 genes did not have any effect on levels of YFP expressed under the same promoter (Supplementary Fig. 1d) and 5 out of 6 of them had no effect on toxicity of α–syn or TDP-43 (Supplementary Fig. 2 a,b and data not shown). One $(PR)_{50}$ toxicity suppressor, *ski8*Δ, also suppressed TDP-43 toxicity (Supplementary Fig. 2a) but had no effect on α–syn toxicity (Supplementary Fig. 2b). These modifiers represent an interesting class, which might regulate expression levels or stability of this DPR specifically. Regulating levels of toxic neurodegenerative disease proteins is emerging as an important way to combat their toxicity. Finally, one modifier, *ubr2*Δ, suppressed toxicity of all three toxic proteins ($(PR)_{50}$, TDP-43, and α–syn). This gene encodes an E3 ubiquitin ligase, perhaps pointing to a common way to mitigate toxicity from diverse aggregation-prone disease proteins.

Immunocytochemistry in yeast cells

For immunocytochemistry yeast was induced in 2% galactose for 5 hours and then fixed with 4% paraformaldehyde for 1 hour at room temperature. Cells were collected by centrifugation, washed twice with PBS, and resuspended in 1ml of solution A (0.5 mM $MgCl_2$, 1.2 M sorbitol, 40 mM K_3PO_4, pH 6.5). To generate spheroplasts we added 10 μl of β-mercaptoethanol and 25 μl if 10 mg/ml lyticase for 15 min at 37°C. Spheroplasted cells were collected by centrifugation, washed once with 1 ml of PBS, once with 1 ml of solution A and resuspeded in 250 μl of PBS+BSA (1× PBS, 1 mg/ml BSA). 150 μl of cell suspension was incubated on Superfrost Plus slides (Fisher) for 5 min and blocked with 50 μl of PBS +BSA for 30 min at room temperature. Cells were then incubated with anti-FLAG antibody (1:100, Sigma #F1804), washed 3 times with PBS, incubated with anti-mouse secondary antibody (1:800, Invitrogen #21203) and washed 3 times with PBS. Samples were mounted using ProLong Gold with DAPI (Life Technologies).

Functional enrichment analysis

Functional enrichment analysis was performed with the Functional Annotation Chart tool of DAVID v. 6.7[24] using the *S. cerevisiae* genome as background[24].

Mouse primary neuron culture

All mouse experiments were performed in compliance with Stanford Administrative Panel on Laboratory Animal Care guidelines and regulations. E17 mouse cortical neurons were

isolated using Papain Dissociation System (Worthington Biochemicals, #LK003150), plated on poly-L-lysine coated plates and grown in neurobasal medium supplemented with B-27 (Invitrogen) and glutamine. At DIV4 neurons were transduced with lentiviruses encoding GFP, $(PR)_{50}$ or KPNA3, under conditions that conferred transduction efficiency of 95%. 5 days post-infection neuronal survival was assessed by NeuN (1:1000, Millipore #MAB377) counting. Experiment assessing the effects of KPNA3 upregulation on $(PR)_{50}$ toxicity in mouse neurons was repeated three independent times. In each experiment, neuronal survival was assessed in minimum 6 separate wells for each condition. All images were obtained and neuronal numbers assessed in a blinded fashion.

Direct conversion of human dermal fibroblasts into induced neurons (iN)

Primary human dermal fibroblasts from 3 healthy control patients and 2 *C9orf72*-ALS patients were obtained from Coriell Institute[25] and the University Hospital Erlangen. Fibroblasts were cultured in DMEM medium containing 15% FBS and 0.1% NEAA (all Gibco). Direct Ngn2 and Ascl1-based conversion was performed similar to previously described[18,26]. Briefly, the cells were lentivirally transduced with pLVX-EtO and pLVXTP-N2A and further passaged in the presence of G418 (200 μg/ml Gibco) and puromycin (1 μg/ml; Sigma-Aldrich) in tetracycline-free FBS-containing media. To generate induced neurons the media was changed to induced neuron conversion media for 3 weeks and changed every 3 days. Induced neuron conversion media is based on DMEM:F12/ Neurobasal (1:1 v/v) and contains the following supplements: N2 supplement and B27 supplement (both 1×; Gibco), doxycycline (2 μg/ml, Sigma-Aldrich), Laminin (1 μg/ml, life technologies), dibutyryl cyclic-AMP (500 μg/ml, Sigma-Aldrich), human recombinant noggin (150 ng/ml; Preprotech), LDN-193189 (0.5 μM; Cayman Chemical Co) and A83-1 (0.5 μM; Stemgent), CHIR99021 (3 μM, LC Laboratories), Forskolin (5 μM, LC Laboratories) and SB-431542 (10 μM; Cayman Chemical Co). For maturation, iN cells were gently transferred on top of a monolayer culture of mouse astrocytes[27] and further cultured for one weeks (4 weeks total) in induced neuron maturation media containing the supplements GDNF, BDNF (both 20 ng/ml, R&D), dibutyryl cyclic-AMP (500 μg/ml, Sigma-Aldrich), doxycycline (2 μg/ml, Sigma-Aldrich) and laminin (1 μg/ml, life technologies) and subsequently fixed with 4% PFA. iNeurons were labelled with anti-RCC1 (1:50, Santa Cruz Biotechnology, #sc-1161), anti-TUJ1 (1:3000, Millipore), anti-lamin B (1:100, Santa Cruz Biotechnology, #sc-6217), RanGAP1 (1:50, Santa Cruz Biotechnology, #sc-25630), anti-exportin 5 (1:100, Bethyl Laboratories, A303-991A), anti-TNPO3 (1:100, Abcam, #ab54353), anti-KPNA3 (1:100, Everest Biotech, #EB06237). All images were obtained and analyzed in a blinded fashion.

Supplementary Material

Refer to Web version on PubMed Central for supplementary material.

Acknowledgments

We thank John Ravits and Clotilde Lagier-Tourenne for sharing the control and *C9orf72* ALS patient fibroblasts used in this study. We acknowledge microscopy assistance from the Stanford Neuroscience Microscopy Service, supported by NIH NS069375. This work was supported by NIH grants 1R01NS065317 and 1R01NS073660 (A.D.G.). A.D.G. is supported by the Packard Center for ALS Research at Johns Hopkins and Target ALS. A.J. is

supported by the Dean's Postdoctoral Fellowship from Stanford University. S.S. is a recipient of NIH K99/R00 Award (NS091538) and Target ALS Springboard Fellowship. J.M. and F.H.G. are supported by J.P.B. Foundation, the Helmsley Foundation, and the Mathers Foundation. Additional research funding was provided by the KU Leuven, the European Research Council in the context of the European's Seventh Framework Programme (FP7/2007–2013 and ERC grant agreement n° 340429), the Fund for Scientific Research Flanders (FWO-Vlaanderen) G.0983.14N, the Interuniversity Attraction Poles Programme P7/16 initiated by the Belgian Science Policy Office, the Association Belge contre les Maladies Neuro-Musculaires (ABMM), the ALS Liga (Belgium) and the 'Opening the Future' Fund. S.B. received a fellowship from the Agency for Innovation by Science and Technology IWT. E.B. holds a post-doctoral fellowship from FWO-Vlaanderen. W.R. is supported through the E. von Behring Chair for Neuromuscular and Neurodegenerative Disorders

References

1. DeJesus-Hernandez M, et al. Expanded GGGGCC hexanucleotide repeat in noncoding region of C9ORF72 causes chromosome 9p-linked FTD and ALS. Neuron. 2011; 72:245–256. [PubMed: 21944778]
2. Renton AE, et al. A hexanucleotide repeat expansion in C9ORF72 is the cause of chromosome 9p21-linked ALS-FTD. Neuron. 2011; 72:257–268. [PubMed: 21944779]
3. Ash PE, et al. Unconventional translation of C9ORF72 GGGGCC expansion generates insoluble polypeptides specific to c9FTD/ALS. Neuron. 2013; 77:639–646. [PubMed: 23415312]
4. Mori K, et al. The C9orf72 GGGGCC repeat is translated into aggregating dipeptide-repeat proteins in FTLD/ALS. Science. 2013; 339:1335–1338. [PubMed: 23393093]
5. Zu T, et al. RAN proteins and RNA foci from antisense transcripts in C9ORF72 ALS and frontotemporal dementia. Proc. Natl. Acad. Sci. U.S.A. 2013; 110:E4968–E4977. [PubMed: 24248382]
6. Mizielinska S, et al. C9orf72 repeat expansions cause neurodegeneration in Drosophila through arginine-rich proteins. Science. 2014; 345:1192–1194. [PubMed: 25103406]
7. Kwon I, et al. Poly-dipeptides encoded by the C9orf72 repeats bind nucleoli, impede RNA biogenesis, and kill cells. Science. 2014; 345:1139–1145. [PubMed: 25081482]
8. Zhang YJ, et al. Aggregation-prone c9FTD/ALS poly(GA) RAN-translated proteins cause neurotoxicity by inducing ER stress. Acta. Neuropathol. 2014; 128:505–524. [PubMed: 25173361]
9. May S, et al. C9orf72 FTLD/ALS-associated Gly-Ala dipeptide repeat proteins cause neuronal toxicity and Unc119 sequestration. Acta. Neuropathol. 2014; 128:485–503. [PubMed: 25120191]
10. Yamakawa M, et al. Characterization of the dipeptide repeat protein in the molecular pathogenesis of c9FTD/ALS. Hum. Mol. Genet. 2014
11. Wen X, et al. Antisense Proline-Arginine RAN Dipeptides Linked to C9ORF72-ALS/FTD Form Toxic Nuclear Aggregates that Initiate In Vitro and In Vivo Neuronal Death. Neuron. 2014; 84:1213–1225. [PubMed: 25521377]
12. Elden AC, et al. Ataxin-2 intermediate-length polyglutamine expansions are associated with increased risk for ALS. Nature. 2010; 466:1069–1075. [PubMed: 20740007]
13. Sun Z, et al. Molecular determinants and genetic modifiers of aggregation and toxicity for the ALS disease protein FUS/TLS. PLoS Biol. 2011; 9:e1000614. [PubMed: 21541367]
14. Armakola M, et al. Inhibition of RNA lariat debranching enzyme suppresses TDP-43 toxicity in ALS disease models. Nat. Genet. 2012; 44:1302–1309. [PubMed: 23104007]
15. Krebber H, Taura T, Lee MS, Silver PA. Uncoupling of the hnRNP Npl3p from mRNAs during the stress-induced block in mRNA export. Genes Dev. 1999; 13:1994–2004. [PubMed: 10444597]
16. Dormann D, et al. ALS-associated fused in sarcoma (FUS) mutations disrupt Transportin-mediated nuclear import. EMBO J. 2010; 29:2841–2857. [PubMed: 20606625]
17. Neumann M, et al. FET proteins TAF15 and EWS are selective markers that distinguish FTLD with FUS pathology from amyotrophic lateral sclerosis with FUS mutations. Brain. 2011; 134:2595–2609. [PubMed: 21856723]
18. Bardy C, et al. Neuronal medium that supports basic synaptic functions and activity of human neurons in vitro. Proc. Natl. Acad. Sci. U.S.A. 2015; 112:E2725–E2734. [PubMed: 25870293]
19. Chew J, et al. C9ORF72 repeat expansions in mice cause TDP-43 pathology, neuronal loss, and behavioral deficits. Science. 2015; 348:1151–1154. [PubMed: 25977373]

20. Haeusler AR, et al. C9orf72 nucleotide repeat structures initiate molecular cascades of disease. Nature. 2014; 507:195–200. [PubMed: 24598541]

Online References

21. Hu Y, et al. Approaching a complete repository of sequence-verified protein-encoding clones for Saccharomyces cerevisiae. Genome Res. 2007; 17:536–543. [PubMed: 17322287]

22. Tong AH, et al. Systematic genetic analysis with ordered arrays of yeast deletion mutants. Science. 2001; 294:2364–2368. [PubMed: 11743205]

23. Collins SR, Schuldiner M, Krogan NJ, Weissman JS. A strategy for extracting and analyzing large-scale quantitative epistatic interaction data. Genome Biol. 2006; 7:R63. [PubMed: 16859555]

24. Huang da W, Sherman BT, Lempicki RA. Systematic and integrative analysis of large gene lists using DAVID bioinformatics resources. Nat. Protoc. 2009; 4:44–57. [PubMed: 19131956]

25. Lagier-Tourenne C, et al. Targeted degradation of sense and antisense C9orf72 RNA foci as therapy for ALS and frontotemporal degeneration. Proc. Natl. Acad. Sci. U.S.A. 2013; 110:E4530–E4539. [PubMed: 24170860]

26. Ladewig J, et al. Small molecules enable highly efficient neuronal conversion of human fibroblasts. Nat. Methods. 2012; 9:575–578. [PubMed: 22484851]

27. Mertens J, et al. Embryonic stem cell-based modeling of tau pathology in human neurons. Am. J. Pathol. 2013; 182:1769–1779. [PubMed: 23499461]

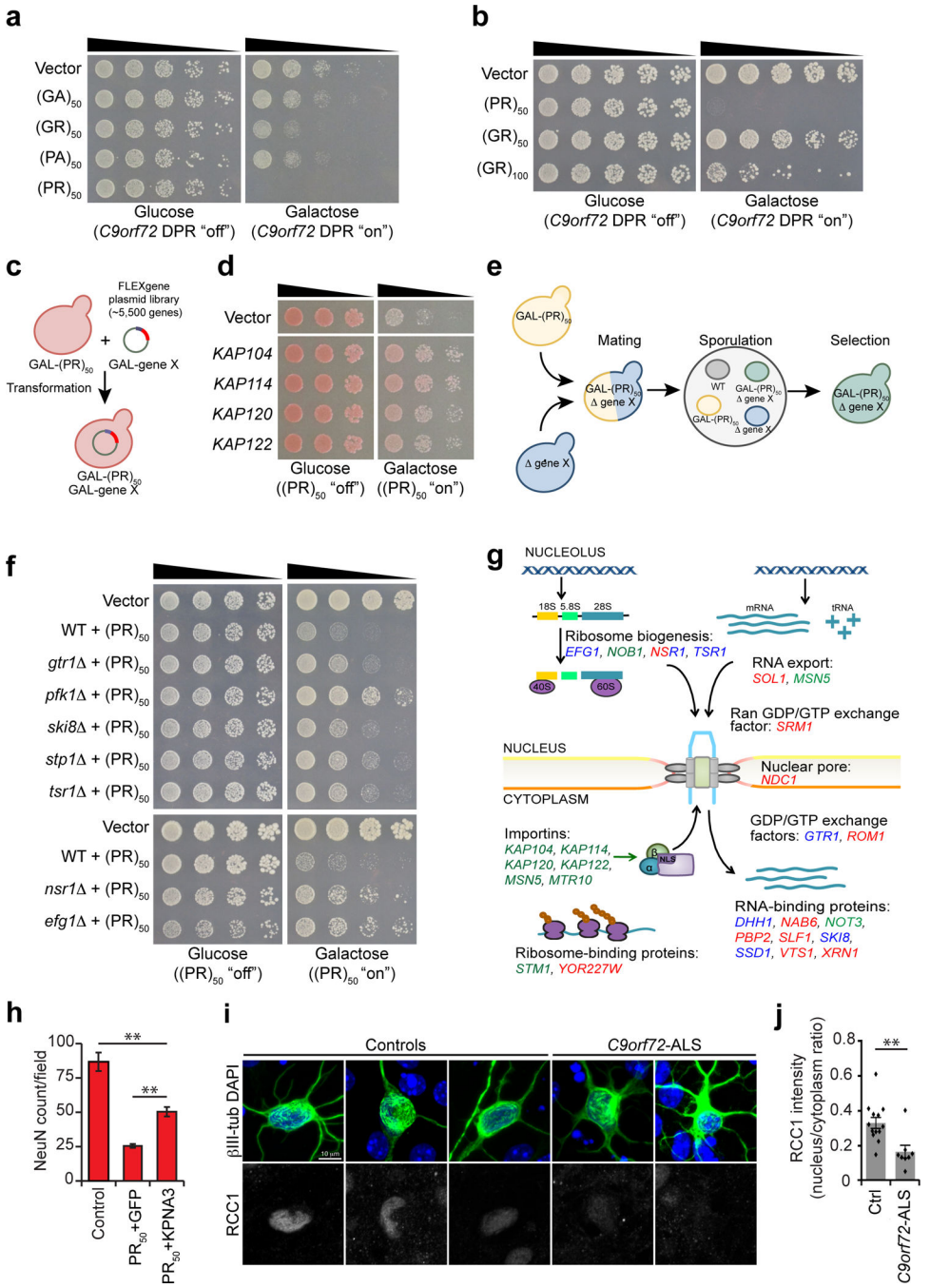

Figure 1.

Yeast screens identify potent modifiers of *C9orf72* DPR toxicity. **a**) Arginine-rich *C9orf72* DPRs are toxic in yeast. Spotting assay demonstrates $(GR)_{50}$ and $(PR)_{50}$ constructs are toxic when expressed in yeast. Galactose was used to induce expression of each DPR construct and glucose was used to repress expression. Five-fold serial dilutions of yeast cells were spotted on glucose- or galactose-containing plates. **b)** $(GR)_{50}$ is less toxic than $(PR)_{50}$ and increasing the DPR length to 100 increased GR toxicity. **c**) Schematic of plasmid overexpression screen to identify genes that suppress or enhance $(PR)_{50}$ toxicity when

overexpressed. **d**) Examples of overexpression suppressors of $(PR)_{50}$ toxicity include members of the karyopherin family of nuclear transport proteins. **e**) Schematic of yeast deletion screen to identify genes that suppress $(PR)_{50}$ toxicity when deleted. **f**) Examples of deletion suppressors of $(PR)_{50}$ toxicity, including *gtr1*Δ, a negative regulator of the Ran-GTPase cycle and *nsr1*Δ, a deletion of the yeast homolog of the human nucleolar protein nucleolin. **g)** A model depicting where the modifier genes from deletion and overexpression screens function. Genes colored blue suppressed toxicity when deleted. Genes colored red enhanced toxicity when overexpressed. Genes colored green suppressed toxicity when overexpressed. **h)** Upregulation of *KPNA3* protects against $(PR)_{50}$ toxicity in rodent neurons. Upregulation of *KPNA3* more than doubled the survival of the neurons expressing $(PR)_{50}$ compared to co-infection with GFP. Graph represents mean ± SEM, n = 6. ** represents p-value <0.01, by unpaired t-test. **i)** *C9orf72*-ALS patient-derived neurons show decreased nuclear localization of RCC1 (human homolog of yeast SRM1) compared to healthy control-derived neurons. **j)** Quantitation of nuclear vs. cytoplasmic fluorescence intensity for RCC1. Human induced neurons from 3 healthy control subjects and 2 *C9orf72*-ALS patients were compared. Graph represents mean ± SEM, n = 13 (healthy controls), n = 8 (*C9orf72*-ALS) ** represents *P* <0.01, by unpaired t-test.

Table 1

List of yeast genes that suppress or enhance $(PR)_{50}$ toxicity when overexpressed.

Yeast Gene	Type	Function	Human Ortholog
Nucleocytoplasmic transport			
KAP104	S2	Karyopherin, nuclear import receptor	TNPO1
KAP114	S2	Karyopherin, nuclear import receptor	IPO9
KAP120	S1	Karyopherin, nuclear import receptor	IPO11
KAP122	S2	Karyopherin, nuclear import receptor	KPNA3
MSN5	S2	Karyopherin, nuclear import and export receptor	XPO5
MTR10	S2	Karyopherin, nuclear import receptor	TNPO3
NDC1	E1	Transmembrane nucleoporin	NDC1
PBS2	E1	MAP kinase kinase	MEK1
SDS22	E2	Regulatory subunit Glc7p	PPP1R7
SOL1	E1	Protein with a possible role in tRNA export	PGLS
SRM1	E1	Nucleotide exchange factor for Gsp1p	RCC1
Ribosome biogenesis and function			
NOB1	S2	Required for cleavage of the 20S pre-rRNA	NOB1
STM1	S2	Ribosome preservation factor during cell stress	–
NSR1	E1	Nucleolar protein required for pre-rRNA processing	NCL
RNA-binding protein			
NOT3	S2	Subunit of the CCR4-NOT complex	CNOT3
NAB6	E1	RNA-binding protein	–
PBP2	E2	Heterogeneous nuclear RNP protein	PCBP4
SLF1	E1	RNA-binding protein, associates with polysomes	LARP1
VTS1	E1	RNA-binding protein containing a SAM domain	–
XRN1	E2	5'-3' exonuclease component of cytoplasmic processing bodies	XRN1
Serine/threonine-protein kinase			
PRR2	S2	Involved in MAP kinase signaling	CHECK1
ELM1	E2	Regulates cellular morphogenesis and cytokinesis	CAMKK2
PSK1	E2	PAS domain-containing kinase	PASK
TOS3	E1	Protein kinase functionally orthologous to LKB1	LKB1
Ubiquitination / proteasome			
PRE4	S2	20S proteasome subunit	PSMB4
UBP10	S2	Nucleolar ubiquitin protease	USP36
ROG3	E1	Alpha-arrestin	–
Mitochondria			
ISU2	S2	Mitochondrial scaffold protein	ISCU
MKS1	E3	Transcriptional regulator	–
MMR1	E1	Outer mitochondria membrane protein	–

Yeast Gene	Type	Function	Human Ortholog
Transcription			
ASK10	S1	RNA polymerase II component	–
CRZ1	S1	Calcineurin-responsive transcription factor	–
DAT1	S2	DNA binding protein	–
PGD1	S1	Subunit of the RNA polymerase II mediator complex	–
HCM1	E2	Forkhead transcription factor	–
RGM1	E1	Putative transcriptional repressor	WT1
SPT6	E1	Nucleosome remodeling proteins	SUPT6H
POG1	E1	Chromatin-associated protein of unknown function	–
Other / Unknown function			
AXL1	S1	Haploid specific endoprotease	IDE
BCK2	S2	Serine/threonine-rich protein involved in PKC1 signaling	–
BUG1	S2	Protein involved in ER to Golgi transport	CENPE
EMP24	S1	Integral membrane component of COPII-coated vesicles	TMED2
FUN19	S2	Non-essential protein of unknown function	RAD51
PLP1	S1	Protein that interacts with chaperonin containing TCP1	TXNDC9
POL32	S1	Third subunit of DNA polymerase delta	–
VRP1	S1	Verprolin, proline-rich actin-associated protein	WIFP1
TIR4	S1	Cell wall mannoprotein	MAGEE1
YHR131C	S2	Putative protein of unknown function	–
ALR2	E1	Probable Mg(2+) transporter	–
BOP3	E1	Protein of unknown function	COBL
CDC6	E2	ATP-binding protein required for DNA replication	CDC6
COS2	E1	Protein of unknown function	–
COS3	E2	Protein involved in salt resistance	–
HER1	E3	Protein of unknown function	SLITRK6
MEP3	E1	Ammonium permease	RHAG
PFK1	E2	Alpha subunit of phosphofructokinase	PFKP
ROM1	E1	GDP/GTP exchange protein (GEP) for Rho1p	RHOA
ROY1	E1	GTPase inhibitor with similarity to F-box proteins	–
SPS22	E1	Protein of unknown function	–
YCL001W-B	E1	Protein of unknown function	PELO
YPR013C	E1	Putative zinc finger protein	–
YTA7	E1	Protein with a role in regulating histone gene expression	ATAD2B

S, suppressor of $(PR)_{50}$ toxicity (S1, moderate; S2, strong)

E, enhancer of $(PR)_{50}$ toxicity (E1, moderate; E2, strong; E3, very strong)

Table 2

List of yeast gene deletions that suppress $(PR)_{50}$ toxicity.

Yeast Gene Deletion	Suppress $(GR)_{100}$ toxicity	Function	Human Ortholog(s)
*dhh1*Δ	yes	Cytoplasmic DExD/H-box helicase; may have a role in mRNA export	DDX6
*efg1*Δ	yes	Nucleolar protein required for maturation of 18S rRNA	–
*gtr1*Δ	no	GTP binding protein, negative regulator of Ran/Tc4 GTPase cycle	RRAGA / RRAGB
*nsr1*Δ	yes	Nucleolar protein required for ribosome biogenesis	NCL
*pfk1*Δ	yes	Alpha subunit of phosphofructokinase involved in glycolysis	PFKP
*sgo1*Δ	not tested	Component of the spindle checkpoint	SGOL1
*ski8*Δ	yes	Protein involved in exosome mediated 3' to 5' mRNA degradation	WDR61
*ssd1*Δ	not tested	Translational repressor, affects mRNA localization	DISL3L2
*stp1*Δ	yes	Activates transcription of amino acid permease genes	–
*tsr1*Δ	yes	Required for 20S pre-rRNA processing in the cytoplasm	TSR1
*uaf30*Δ	yes	Subunit of UAF (upstream activation factor) complex	SMARCD1
*ubr2*Δ	yes	Cytoplasmic ubiquitin-protein ligase (E3)	UBR1
*vma16*Δ	yes	Subunit of the vacuolar ATPase; vacuole acidification	ATP6V0B
*ypt6*Δ	yes	Rab family GTPase involved in the secretory pathway	RAB6
*ykl151c*Δ	not tested	NADHX dehydratase; converts (S)-NADHX to NADH	CARKD
*ynl198c*Δ	yes	Unknown function	–